

3D SULFONATED GRAPHENE HYDROGEL FOR ENHANCED CHEMICAL SENSING

Jin Wu¹, Kai Tao¹, Di Chen³, Jianmin Miao¹ and Leslie K. Norford²

¹School of Mechanical and Aerospace Engineering, Nanyang Technological University, Singapore

²Massachusetts Institute of Technology, USA

³Shanghai Jiao Tong University, P.R. China

ABSTRACT

One-step, hydrothermal synthesized 3D sulfonated reduced graphene oxide hydrogel (S-RGOH) is employed to fabricate a chemical sensor with high sensitivity, good selectivity, fast response and reversibility toward several gases. Compared with unmodified RGOH counterparts, the 3D NaHSO₃ functionalized S-RGOH sensor exhibits 61.3 and 58.9 times higher responses to NO₂ and NH₃, respectively. A low limit of detection (LOD) of 4.1 ppb and 1.48 ppm for NO₂ and NH₃, respectively, has been achieved. The sensor exhibits fast and complete recovery at room temperature. Importantly, for the first time, the characteristics of a linear fitted response-temperature relationship are exploited to discriminate many different gases. An integrated microheater is deployed to modulate substrate temperature rapidly with low power consumption.

INTRODUCTION

NO₂, mainly released by combustion of fossil fuels, may cause acid rain, photochemical smog and respiratory problems in humans [1]. Ammonia (NH₃), mainly emitted from agricultural process, is also a toxic gas. Detection of air polluting gaseous chemicals such as NO₂ and NH₃ is important not only to the health of human being, but also to the environment protection [2]. Graphene has proved to be a promising candidate in chemical sensing due to its atom-thick 2D structure, high surface area, excellent electronic conductivity, low electrical noise and high sensitivity to electrical perturbations from gas molecules [3]. Although reduced graphene oxide (RGO) has attracted intensive research interest due to the high-yield, cost-effective production and facile chemical modification, pristine RGO exhibits limited sensing performance to gaseous chemicals, such as low sensitivity, poor selectivity and sluggish signal recovery [4]. 3D structural design and surface chemical modification of RGO are effective routes toward improved sensitivity. The 3D porous graphene not only provides increased surface interaction area and defect sites to enhance the gas molecules adsorption, but also gives an alternative path for the transport of charge carriers through the nanoscale pores [5, 6]. Chemical modification of graphene can also enhance the sensitivity due to the strong interaction between the doped functional groups and gas molecules. For example, a first-principles theoretical study indicates that S-doped graphene can form a strong binding with NO₂ molecules [7].

In this work, we combine the 3D structural engineering and chemical modification of RGO to develop a gas sensor based on 3D sulfonated reduced graphene oxide hydrogel (S-RGOH), which is employed to detect various gases with enhanced performance. Compared with

its unmodified RGOH counterparts, the S-RGOH exhibits 61.3 and 58.9 times higher responses to 6 ppm NO₂ and 200 ppm NH₃, respectively. In addition, the 3D S-RGOH sensor displays a much lower limit of detection (LOD) compared with unmodified RGOH counterpart. Graphene-based gas sensors suffer from poor selectivity because different gas molecules may adsorb on the same RGO flake surface and change its resistance. However, we have employed temperature dependent response characteristics of RGO for different gases to differentiate these gases chemicals. This leads to an improved selectivity for each detectable gas.

EXPERIMENTAL METHODS

Graphene oxide (GO) was synthesized from graphite powder using the modified Hummers' method [5]. For the synthesis of S-RGOH, 42 mg NaHSO₃ was added into 10 mL of 2 mg/mL aqueous suspension of GO. The mixed suspension was heated at 95 °C for 3 h in an autoclave. The synthesis procedures of unmodified RGOH were described in our previous work [5]. After reaction, the solid S-RGOH was centrifuged and washed several times with DI water to remove unreacted NaHSO₃. Subsequently, the solid S-RGOH was redispersed in water to prepare a uniform 2 mg/mL aqueous dispersion of S-RGOH by ultrasonication.

The morphology of materials was characterized by FE-SEM 7600. X-ray powder diffraction (XRD) spectra of the prepared S-RGOH were obtained by a Bruker D8 advance X-ray diffractometer. Raman spectra of samples were acquired using a spectrophotometer (alpha300 R from WITec) with a 514 nm laser. A Kratos XSAM 800 spectrometer with an Mg K α (1253.6 eV) X-ray source was employed to obtain the X-ray photoelectron spectroscopy (XPS) spectra.

The Au interdigital electrodes (IEs) and microheater were fabricated by micromachining technologies on the front and back sides of the Si/SiO₂ wafer (300 μm thick Si with 260 nm thick SiO₂ layers on both sides), respectively. The serpentine Pt heating lines on the microheater had a width of 25 μm and the thickness of 300 nm. The Au strips on the IEs had the width and gap of 20 μm. The 2 mg/mL aqueous dispersion of S-RGOH was drop casted on the Au IEs. After evaporation of water, the solid 3D S-RGOH bridged the gaps on the IEs. The resistance of the sensor was recorded by a Keithley 2602 Source Meter when a fixed bias voltage of 0.1 V was applied on the two electrodes of IEs.

RESULTS AND DISCUSSION

Material Characterization

A facile, one-step hydrothermal method is employed to synthesize the 3D S-RGOH (Figure 1a) [8]. The

NaHSO_3 can facilitate the reduction and self-assembly of GO simultaneously in the hydrothermal process, making the reaction finish at low temperature ($<100^\circ\text{C}$). The SEM image in Figure 1a (right) exhibits the 3D porous morphology of the synthesized 3D S-RGOH. The pore size ranges from several nanometers to micrometers. The XRD peak positions of S-RGOH were consistent with the characteristic peak positions of RGO, confirming the successful formation of RGO in the hydrothermal process (Figure 2a). From the XRD patterns, the interlayer spacing of S-RGOH is calculated to be 3.76 \AA , which is much smaller than that of GO (6.95 \AA), but a little larger than that of graphite (3.35 \AA), demonstrating the existence of π - π stacking between RGO sheets in S-RGOH. A D-band (1343 cm^{-1}) and a G-band (1593 cm^{-1}) appear on the Raman spectra of GO and S-RGOH (Figure 2b). The increased ratio of I_D/I_G from GO to S-RGOH is attributed to the increased surface functional groups and defective sites on the carbon basal plane. The XPS spectra in Figure 2c demonstrate that S-RGOH is composed of C, O, S and Na, while the unmodified RGOH only consists of C and O, indicating that NaHSO_3 successfully modified the S-RGOH surface. The XPS quantitative elemental analysis demonstrates that the ratios of C/O and C/S were 3.1 and 20.2 respectively, suggesting that nearly 20 C atoms were decorated with one HSO_3^- group. The measured current versus voltage (I - V) curves in Figure 2d demonstrate GO is nearly non-conductive, while the S-RGOH is conductive. This demonstrates the efficient de-oxygenation and reduction of GO in the hydrothermal synthesis process. The S-RGOH and RGOH based sensors have the resistance of 376 and $37\text{ K}\Omega$, respectively. The increased resistance of S-RGOH compared with RGOH is attributed to the surface modification of NaHSO_3 molecules. In addition, the linear I - V relationship demonstrates the ohmic contact between graphene and the Au IEs. The low-resistance electrical contact enables the evaluation of the intrinsic sensing performance of the S-RGOH. The microheater was fabricated on the back side of the sensor substrate (Figure 1b). Due to the local heating effect, the microheater can raise substrate temperature rapidly with little power consumption and small device size. The SEM image in Figure 1c shows the serpentine morphology of the Pt heating lines on the microheater.

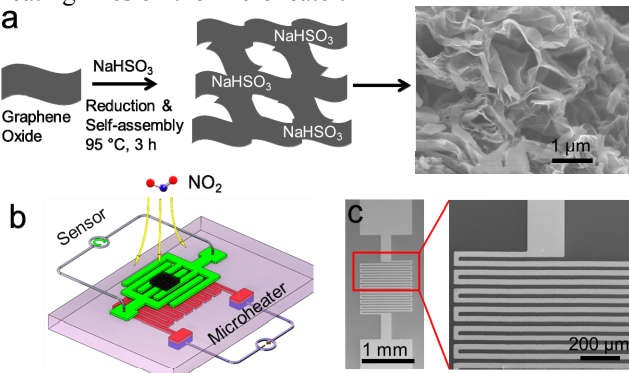


Figure 1: (a) Synthesis of 3D S-RGOH in a one-step hydrothermal self-assembly process. (b) Scheme illustrating the structure of the device. The 3D graphene bridged IEs were fabricated on the front side of the substrate, and the microheater was produced on the back

side. (c) SEM images of the microheater and the magnified Pt heating lines on the microheater.

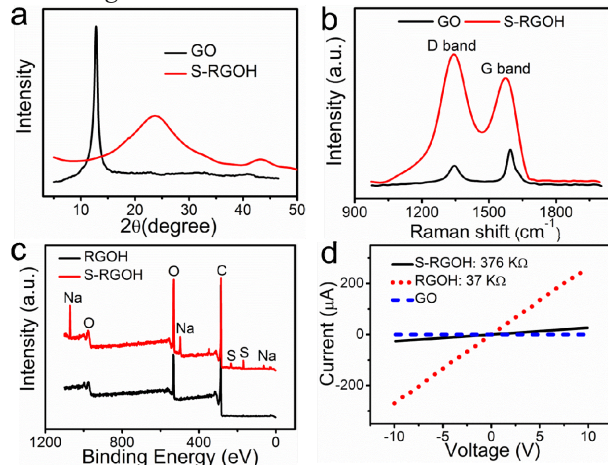


Figure 2: (a) XRD spectra of GO (black) and S-RGOH (red). (b) Raman spectra of GO (black) and S-RGOH (red). (c) XPS survey scan spectra of RGOH (black) and S-RGOH (red). (d) I - V curves of GO (blue), RGOH (red) and S-RGOH (black).

Gas Sensing Performance

The gas sensing property of S-RGOH sensor was evaluated by the normalized resistance change upon exposure to a test gas. The normalized resistance is defined as $R/R_0\text{ (\%)}$ and the response is defined as: $(R_0-R)/R_0\text{ (\%)} = \Delta R/R_0\text{ (\%)}$, in which R_0 and R are the resistances before and after exposure of the sensor to a test gas, respectively. The S-RGOH sensor showed a significant and fast resistance reduction upon exposure to NO_2 (Figure 3a). Furthermore, the response increased monotonically from 82.1% for 6 ppm NO_2 to 166.3% for 20 ppm. It is worth noticing that the S-RGOH exhibits 61.3 times higher responses to 6 ppm NO_2 compared with its unmodified RGOH counterpart, demonstrating the important role of chemical modification in boosting the sensitivity. Importantly, a linear relationship between response and NO_2 concentration was observed (Figure 3b). This linear relationship is advantageous for the practical application of the gas sensor. The sensitivity (slope of linearly fitted response line) of this 3D S-RGOH sensor was calculated to be 8.69 ppm^{-1} , which was not only 65.3 times larger than that of an RGOH sensor (0.133 ppm^{-1}), but also higher than those of most of reported graphene-based NO_2 sensors. The LOD of a sensor can be obtained when the signal level is three times larger than the noise level. From the linearly fitted response relationship and the calculated noise level, the theoretical LOD can be calculated to be as low as 4.1 ppb, which was much lower than that of the unmodified RGOH counterpart (178 ppb). To study the stability, the S-RGOH based sensor was employed to detect 4 ppm NO_2 for three successive cycles (Figure 3c-d). The response was nearly constant in the three sensing cycles. A small response variation of 2.54% indicates the good repeatability of this sensor. To study the signal response and recovery speed, the time needed to achieve 50% of its steady response is defined as the response time t_{50} , and the time spent to reach 90% signal recovery after a sensing event is defined as the recovery time t_{90} . As such, the t_{90} is calculated to be as short

as 11 s, demonstrating the fast signal recovery. Note that 90% signal recovery occurred at room temperature, revealing the good reversibility. This S-RGOH based NO₂ sensor is different from those of RGO and carbon nanotube-based NO₂ sensors, which usually need UV light or heating to facilitate recovery [4].

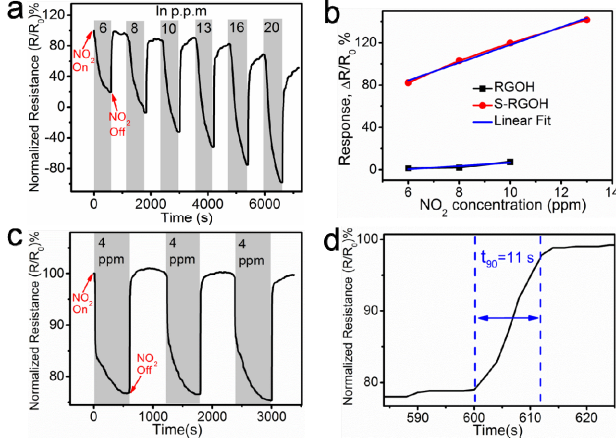


Figure 3: (a) Dynamic response of the S-RGOH sensor to 6-20 ppm NO₂. (b) Plot of the response versus NO₂ concentration for the S-RGOH and RGOH sensors. (c) Dynamic response of the S-RGOH sensor upon exposure to 4 ppm NO₂ in three consecutive sensing cycles. (d) Analysis of the recovery time t_{90} in 4 ppm NO₂ detection.

In addition to NO₂, this 3D S-RGOH sensor also displays good response to NH₃ (Figure 4a). Contrary to NO₂ sensing, the resistance of the S-RGOH sensor increased rapidly upon exposure to NH₃. This is attributed to the electron-donating characteristic of NH₃ molecules, which is different from the electron-withdrawing nature of NO₂. Note that the S-RGOH sensor displayed 58.9 times larger response than that of unmodified RGOH counterpart (Figure 4b). The response increased monotonically with increased NH₃ concentration. Furthermore, a nearly linear relationship between response and NH₃ concentration was obtained. From the linear fitted response versus NH₃ concentration line, the theoretical LOD of NH₃ detection can be extrapolated as low as 1.48 ppm. Furthermore, NH₃ with the low concentration of 20 ppm can also be detected by our sensor with a good response of 7.1% (Figure 4c). These results collectively demonstrate the capability of this S-RGOH sensor to detect NH₃ with low concentration. The detection levels for NO₂ with the concentration less than 3 ppm and NH₃ with the concentration lower than 25 ppm are important for practical gas sensors [2]. Apparently, this S-RGOH sensor can detect NO₂ and NH₃ with the concentrations much lower than the criteria. Analysis of the response of the S-RGOH sensor to 20 ppm NH₃ reveals a short response time t_{50} of 16 s. This indicates a faster response of this NH₃ sensor than those of other Gr/RGO based NH₃ sensors (Figure 4d).

The resistance change of the sensor upon exposure to test gas is attributed to a charge transfer process between S-RGOH and gas. Graphene displays a p-type behavior with holes as the charge carriers. When the oxidizing and electron-withdrawing NO₂ molecules adsorb on S-RGOH surface, the holes transfer from NO₂ to S-RGOH increases the carrier (hole) concentration, leading to a reduced

resistance. On the contrary, the hole depletion in S-RGOH upon adsorption of electron-donating NH₃ molecules leads to an increased resistance. The improved response of the S-RGOH sensor compared with its unmodified counterpart is ascribed to the strong interaction between sulfonated functional groups and NO₂ and NH₃ molecules. The HSO₃⁻ is an electron-rich functional group with many lone pairs of electrons. The electron-withdrawing NO₂ molecules tend to adsorb on electron-rich sites of HSO₃⁻ groups and therefore withdraw electrons from S-RGOH, reducing its resistance. The first principles study performed by Dai et al. also indicates that S-doped graphene can bind NO₂ strongly due to large adsorption energy [7]. The boosted response of the S-RGOH sensor to NH₃ compared with unmodified RGOH is attributed to the chemical reaction between sulfonic groups and NH₃, forming ammonium salts. In addition to strong reactive sites, weak interactions, including hydrogen bonding, dipole/dipole and dispersive forces also enhance the interaction between S-RGOH and gas molecules. The 3D porous structures of S-RGOH also promote the sensitivity because the pore filling of gas molecules causes increased interaction surface areas. In addition, the hopping of charge carriers across the nanoscale pores provides alternative paths for charge transport, increasing the signal. In addition to NO₂ and NH₃, the S-RGOH sensor also displays high sensitivity to a variety of volatile organic compounds (VOCs) (Figure 5).

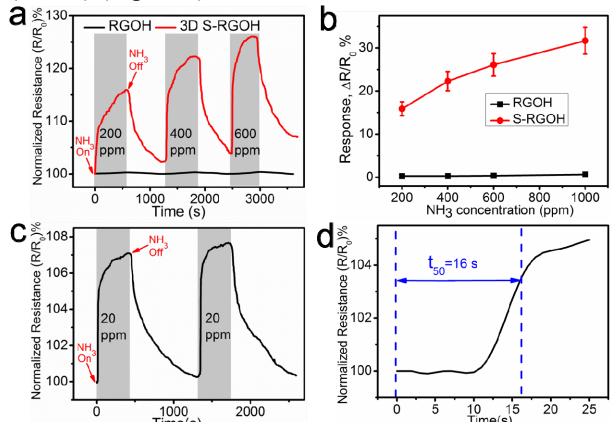


Figure 4: (a) Dynamic responses of the S-RGOH and RGOH sensors to 200-600 ppm NH₃. (b) Plots of response versus NH₃ concentration for the S-RGOH and RGOH sensors. (c) Response of the S-RGOH sensor to 20 ppm NH₃ in two successive cycles. (d) Analysis of the response time t_{50} of the S-RGOH sensor in 20 ppm NH₃ detection.

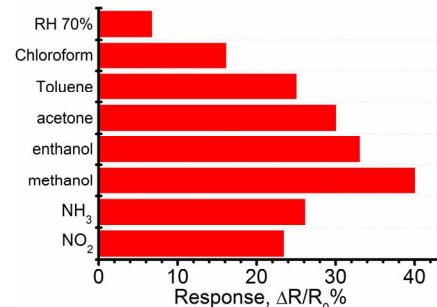


Figure 5: Responses of the S-RGOH sensor to various gaseous chemicals, including NO₂ (4 ppm), NH₃ (600 ppm), saturated methanol, ethanol, acetone, toluene, chloroform

vapors and 70 % RH.

Boosted Selectivity by Microheater

Although the S-RGOH sensor shows good response to various gaseous chemicals, the characteristics of the linear fitted response versus temperature curves can be exploited to distinguish these gases (Figure 6 and Table 1). Due to different binding energy of these gases molecules with graphene, the responses to different gases change in different way with elevated temperature. For NO₂ sensing, the response increased slightly with the elevated temperature from 22 to 45 °C, from which the response-temperature relationship could be linearly fitted as $R = 0.11T + 8.8$ (Figure 6a and d). On the contrary, the responses to NH₃, ethanol and water reduced with temperature (Figure 6b-d). Thus, the response versus temperature curves for NH₃, ethanol and 70% RH detection were linearly fitted as $R = -0.41T + 35$, $R = -0.2T + 37$ and $R = -0.17T + 11$ respectively. It is clear that the slopes and intercepts on the linearly fitted response lines for these four different chemicals are totally different (Table 1). These differences can be employed to discriminate these gaseous chemicals effectively. The temperature of the sensor can be modulated quickly (< 60 s) by programming the voltage applied on the microheater, making it convenient to sweep the temperature to see the response changing trend.

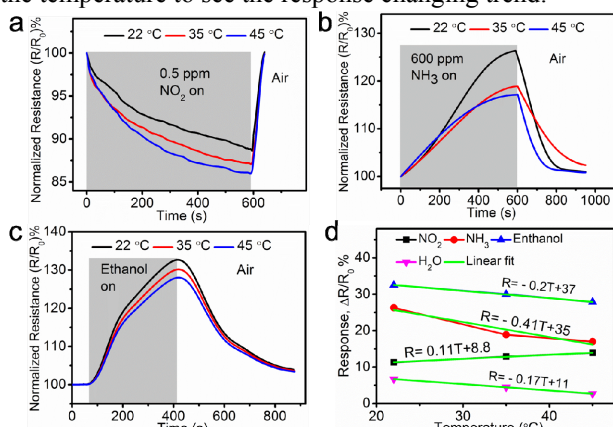


Figure 6: (a), (b) and (c) Responses of this S-RGOH sensor to NO_2 (0.5 ppm), NH_3 (600 ppm) and ethanol (3.8 ppb) at 22, 35 and 45 °C respectively. (d) Plots of experimental obtained and linearly fitted responses of this sensor to NO_2 (0.5 ppm), NH_3 (600 ppm), ethanol (3.8 ppb) and 70 % RH as a function of temperature.

Table 1: Linear fitted response-temperature relationships for different gases

	Linear fitted equation	Slope	Intercept
NO_2	$R = 0.11T + 8.8$	0.11	8.8
NH_3	$R = -0.41T + 35$	-0.41	35
Ethanol	$R = -0.2T + 37$	-0.2	37
H_2O	$R = -0.17T + 11$	-0.17	11

CONCLUSIONS

3D sulfonated RGOH is employed to fabricate a chemiresistor-type gas sensor that exhibits improved sensitivity, good selectivity, fast response and reversibility toward several gases. The sensitivity to various gases chemicals is boosted significantly by chemical modification of graphene with NaHSO₃ molecules and 3D

structural engineering. Importantly, the selectivity of detecting various gases is improved by the imbedded microheater. For the first time, the features on the fitted response-temperature curves are deployed to distinguish different gases. This work provides new insight in improving the performance of graphene-based gas sensors by combining structural design, surface chemical modification and temperature modulation.

ACKNOWLEDGMENTS

This research is supported by the National Research Foundation Singapore under its Campus for Research Excellence and Technological Enterprise programme. The Center for Environmental Sensing and Modeling is an interdisciplinary research group of the Singapore MIT Alliance for Research and Technology.

REFERENCES

- [1] W. Yuan, L. Huang, Q. Zhou, and G. Shi, "Ultrasensitive and selective nitrogen dioxide sensor based on self-assembled graphene/polymer composite nanofibers," *ACS Appl. Mater. Interfaces*, vol. 6, pp. 17003-17008, 2014.
- [2] L. T. Duy, D.-J. Kim, T. Q. Trung, V. Q. Dang, B.-Y. Kim, H. K. Moon, *et al.*, "High Performance Three-Dimensional Chemical Sensor Platform Using Reduced Graphene Oxide Formed on High Aspect-Ratio Micro-Pillars," *Adv. Funct. Mater.*, vol. 25, pp. 883-890, 2015.
- [3] J. Wu, K. Tao, J. Zhang, Y. Guo, J. Miao, and L. K. Norford, "Chemically functionalized 3D graphene hydrogel for high performance gas sensing," *J. Mater. Chem. A*, vol. 4, pp. 8130-8140, 2016.
- [4] W. Yuan, A. Liu, L. Huang, C. Li, and G. Shi, "High-performance NO_2 sensors based on chemically modified graphene," *Adv. Mater.*, vol. 25, pp. 766-771, 2013.
- [5] J. Wu, K. Tao, J. Miao, and L. K. Norford, "Improved Selectivity and Sensitivity of Gas Sensing Using a 3D Reduced Graphene Oxide Hydrogel with an Integrated Microheater," *ACS Appl. Mater. Interfaces*, vol. 7, pp. 27502-27510, 2015.
- [6] J. Wu, S. Feng, X. Wei, J. Shen, W. Lu, H. Shi, *et al.*, "Facile Synthesis of 3D Graphene Flowers for Ultrasensitive and Highly Reversible Gas Sensing," *Adv. Funct. Mater.*, 2016. DOI: 10.1002/adfm.201603598
- [7] J. Dai, J. Yuan, and P. Giannozzi, "Gas adsorption on graphene doped with B, N, Al, and S: A theoretical study," *Appl. Phys. Lett.*, vol. 95, p. 232105, 2009.
- [8] W. Chen and L. Yan, "In situ self-assembly of mild chemical reduction graphene for three-dimensional architectures," *Nanoscale*, vol. 3, pp. 3132-3137, 2011.

CONTACT

*Jin Wu; tel: +65-83007570; jwu6@e.ntu.edu.sg